

# Electron density in the F region derived from GPS/MET radio occultation data and comparison with IRI

Klemens Hocke and Kiyoshi Igarashi

*Communications Research Laboratory, Tokyo, Japan*

(Received October 22, 2001; Revised September 4, 2002; Accepted September 15, 2002)

The inversion of electron density from total electron content (TEC) measurements of GPS radio occultation is investigated by means of simulated data from the International Reference Ionosphere IRI-2001 and observations by the GPS/MET satellite experiment. In both cases a meridional slice of electron density is derived for northern summer solstice June/July 1995 from the midnight to the noon sector of the Earth's ionosphere. By means of the simulated occultation data a new 2-D recovery method is tested considering electron density variations along the ray path through a non-spherical ionosphere. This method is as fast as the Abel inversion. The relative retrieval error is less than a few percent around and beyond the  $F_2$ -layer peak. The resolution (in latitude) of the 2-D recovery method is significantly better than those of the Abel inversion which assumes spherical symmetry of the ionosphere along the ray path. After this simulation test, the 2-D recovery method and the Abel inversion are applied to the noon-midnight GPS/MET data in June/July 1995, near to solar minimum. The advantages of the 2-D recovery method are in case of the GPS/MET observations questionable. This could be due to data gaps and TEC errors disturbing the 2-D recovery method more than the robust Abel inversion. Finally meridional slices are derived for other local times by the Abel inversion. Because of missing data and uncertainty of possible retrieval errors the discussion of the diurnal and global variations of the F region is confined to the most significant features. Clear departures between GPS/MET and IRI are found for the polar winter ionosphere and the nighttime topside ionosphere at low latitudes. Generally the GPS/MET observations and the IRI predictions agree well for most local times and latitude regions.

## 1. Introduction

The radio occultation or limb sounding technique and the fundamentals of the global positioning system (GPS) are described in numerous articles, reports and books (e.g., Rocken *et al.*, 1997; Lee *et al.*, 2001; Melbourne *et al.*, 1994; Kaplan, 1996). The measurement configuration is depicted in Fig. 1. Remote sensing of the Earth's atmosphere, ionosphere, and oceans by intersatellite links has been rapidly developed since the successful GPS/MET radio occultation mission in 1995–1997. Several new missions are already in orbit (e.g., Oerstedt, SAC-C, CHAMP, GRACE, C/NOFS) or in preparation for launch (e.g., FEDSAT, EQUARS, COSMIC, ACE+). In addition there are some activities, not only to use the decimeter radio waves of GPS but also other wave lengths (e.g., centimeter) which are more sensitive for the measurement of the atmospheric composition (Yakovlev *et al.*, 1995). The GPS signals seem to be ideal for active sounding of neutral density and temperature at tropospheric and stratospheric heights and electron density in the ionosphere. Especially the radio occultation data can provide atmospheric profiles of high vertical resolution (1 km to 100 m), mainly depending on the data analysis method (Mortensen *et al.*, 1999). There are still some obstacles for the retrieval of electron density profiles from occulta-

tion data, since the ionospheric refractivity profile is not so simple as the neutral refractivity profile which exponentially decreases with increase of height and decrease of air density. In case of the neutral refractivity profile the refraction of the GPS signal mainly occurs within the ray path segment around the tangent point (point of closest approach of the ray to the earth center).

Ionospheric refraction of the signal can be significant in all ray path segments, and 'horizontal variations' of the ionosphere over distances of several thousand kilometers should be considered. In the present study we describe the electron density as function of radial distance and geographic position (latitude, longitude). With 'horizontal variation' we always refer to latitudinal and longitudinal variations of electron density at constant radial distance (within a spherical layer as shown in Fig. 1). There are several approaches for analysis of ionospheric occultation data. Firstly, one can ignore horizontal variations. In Section 4 (Abel Inversion) and later it is shown that the Abel inversion completely smooths out linear horizontal gradients of the ionosphere enabling a correct retrieval of electron density. However in case of horizontal variations with quadratic dependences (e.g., peaks or valleys of electron density) the Abel inversion gives slight electron density errors of around 10–30% (Hajj *et al.*, 2000). Instead of the practical Abel inversion, other techniques such as constrained Abel inversion, tomographic solution, and ionospheric data assimilation can be used for occultation

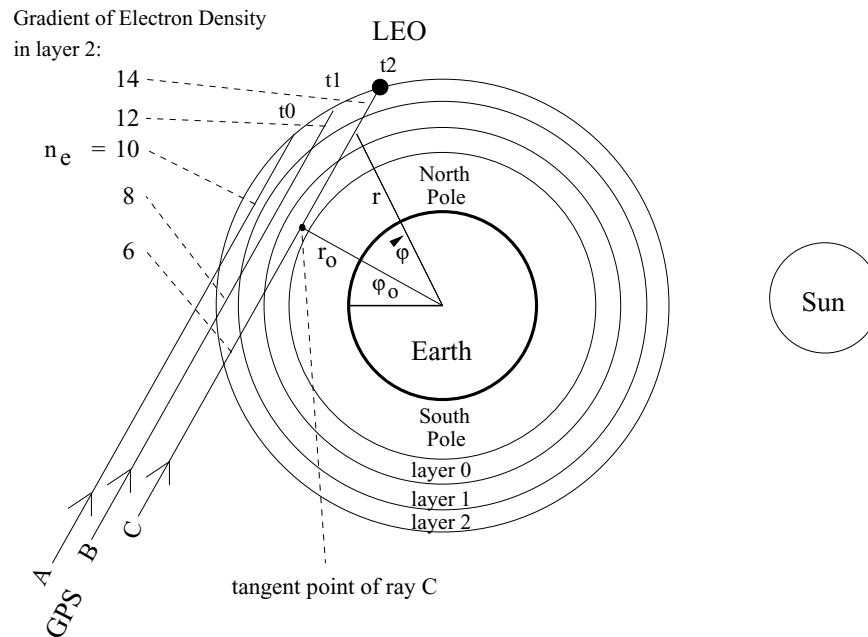


Fig. 1. Measurement configuration for a radio occultation event taking place on the midnight side at latitude  $\phi_0$ . A GPS receiver onboard of the low earth orbit (LEO) satellite observes total electron content along the GPS rays A, B, and C which are received at times  $t_0$ ,  $t_1$ , and  $t_2$ . Electron density variations inside an ionospheric layer (as indicated for layer 2) should be considered for a precise recovery of electron density from total electron content.

data analysis. These techniques have been described and applied by Hajj *et al.* (2000), Schreiner *et al.* (1999), Leitinger *et al.* (1997), Rius *et al.* (1998), and Dymond and Thomas (2001).

The missing knowledge on the variation of the ionosphere along the ray path is obtained from empirical or physical model ionospheres and/or other observations (e.g., simultaneous observations of vertical total electron content by the world-wide network of GPS ground receivers). In case of a single satellite experiment such as GPS/MET, tomographic solutions and data assimilation into 4-D models are handicapped since there are only a few hundred occultation profiles available, scattered over the whole globe and over 24 hours. However the temporal and spatial ionospheric pattern caused by a strong geomagnetic storm has been successfully described by Hernández-Pajares *et al.* (1998) using spaceborne GPS/MET data, GPS ground station data, a grid size of  $10 \times 10$  degrees, eight ionospheric layers, and one hour time resolution.

In the following we try a different way and derive the average behavior of the ionosphere for noon and midnight at northern summer solstice. We solely use the GPS/MET radio occultation data of 2–3 weeks in June/July 1995 and sort the occultation profiles (occurring between 10–14 LT and 22–2 LT) as function of geomagnetic latitude. The TEC values can be easily inverted into a slice of electron density by a 2-D recovery method. Contrary to other techniques such as model-assisted tomography and data assimilation, the 2-D recovery method is not appropriate for real time monitoring of the ionosphere, but it may play a role for discovery, reduction, and analysis of regular ionospheric phenomena and improvement of ionospheric climatologies. It is remarkable that this data analysis method takes into account the horizontal variation of the ionosphere along the ray path with-

out any ‘help from outside’ (physical or empirical models, other observations). This ‘help from outside’ can introduce systematic biases, and comparisons between different observation techniques and ionospheric models become difficult. In the following we firstly test and analyse the 2-D recovery method and the Abel inversion by means of the International Reference Ionosphere IRI-2001 (Bilitza, 2001) before we apply both methods to the real GPS/MET occultation data around noon and midnight. Because of enhanced data gaps, we will only use the Abel inversion for derivation of electron density slices at other local times.

## 2. 2-D Recovery Method

The GPS receiver onboard of the Microlab-1 satellite in a polar orbit ( $70^\circ$  inclination) and in the upper ionospheric F region (730 km orbit height) mainly observes radio occultations of GPS satellites in backward flight direction. The GPS-LEO signal path slices vertically through the atmosphere, and the phase paths of the GPS L1 and L2 signals are recorded by the GPS receiver. The phase path difference is related to the total electron content  $T$  along the ray path (Schreiner *et al.*, 1999)

$$\begin{aligned} T(r_o) &= -\frac{f_1^2}{40.3} S_1(r_o) + k_1 = -\frac{f_2^2}{40.3} S_2(r_o) + k_2 \\ &= \frac{f_1^2 f_2^2}{40.3(f_1^2 - f_2^2)} (S_1(r_o) - S_2(r_o)) + k. \end{aligned} \quad (1)$$

Units are [electrons/m<sup>2</sup>] for  $T$ , [Hz] for GPS L1 and L2 frequencies,  $f_1 = 1.57542$  GHz and  $f_2 = 1.22760$  GHz, and [m] for phase path excess  $S_1$  and  $S_2$ .  $r_o$  denotes the radial distance of the ray perigee (tangent point). The constants  $k_1$ ,  $k_2$ , and  $k$  are related to the signal phase ambiguity and can be removed by a calibration of the retrieved electron density profile at the top and/or bottom of the ionosphere.

In case of GPS/MET the atmospheric phase path excess has been derived by means of a fiducial network of GPS ground receivers and the double difference method (Schreiner *et al.*, 1998).

For the 2-D recovery method it is necessary to have a full latitude-height cross section of TEC values  $T(r_o, \varphi_o, \delta_o)$  where  $\varphi_o$  denotes the latitude position of the occultation event, and  $\delta_o$  the viewing angle (angle between the meridian plane and the GPS ray at the tangent point). The measurement scheme is depicted in Fig. 1 for a radio occultation within the meridian plane. The angles  $\varphi$  and  $\varphi_o$  are counted from the equator of the midnight-side. The south pole is at  $-90^\circ$  (or  $270^\circ$ ), the night-side equator at  $0^\circ$ , the north pole at  $90^\circ$ , and the noon-side equator is at  $180^\circ$ . The total electron content  $T(r_o, \varphi_o, \delta_o)$  is equal to the integrated electron density along the ray with viewing angle  $\delta_o$  and tangent point at radial distance  $r_o$  and latitude position  $\varphi_o$

$$T(r_o, \varphi_o, \delta_o) = \int_{r_o}^{r_{\text{top}}} \frac{r n_e(r, \varphi_-)}{\sqrt{r^2 - r_o^2}} dr + \int_{r_o}^{r_{\text{top}}} \frac{r n_e(r, \varphi_+)}{\sqrt{r^2 - r_o^2}} dr. \quad (2)$$

The first integral is for the integration of electron density from the tangent point in direction to the GPS satellite, while the second integral is equal to the total electron content between tangent point and the LEO satellite. The relation between  $\varphi$ , the integration variable  $r$ , and the viewing angle  $\delta$  is for a straight line

$$\begin{aligned} \varphi_-(r, \delta) &= \varphi_o - \arctan \frac{\sqrt{r^2 - r_o^2} \cos \delta}{r_o} \\ \varphi_+(r, \delta) &= \varphi_o + \arctan \frac{\sqrt{r^2 - r_o^2} \cos \delta}{r_o}. \end{aligned} \quad (3)$$

The equation (2) can be written in a recursive formulation for electron density at the tangent point

$$n_e(r_o, \varphi_o) = \frac{T(r_o, \varphi_o, \delta_o) - \int_{r_1}^{r_{\text{top}}} \frac{r (n_e(r, \varphi_-) + n_e(r, \varphi_+))}{\sqrt{r^2 - r_o^2}} dr}{2r_o(r_1 - r_o)(r_1^2 - r_o^2)^{-1/2}} \quad (4)$$

where  $r_1$  is the radial distance of the layer just above the tangent point layer. The denominator is equal to the ray path segment within the tangent point layer. For higher numerical precision, following expression is used for the square root in the integral

$$\begin{aligned} \frac{\Delta r_k}{\sqrt{r_k^2 - r_o^2}} &= \ln \left| r_{k-1} + \sqrt{r_{k-1}^2 - r_o^2} \right| \\ &\quad - \ln \left| r_k + \sqrt{r_k^2 - r_o^2} \right|, \end{aligned} \quad (5)$$

where  $k = 1, 2, 3, \dots$  indicates the layers beyond the tangent point layer (Steiner, 1998).

Using the recursive formulation in Eq. (4) the TEC values  $T(r_o, \varphi_o, \delta_o)$  can be transformed to the electron density values  $n_e(r_o, \varphi_o)$  within the meridian plane. For this purpose

we start at the top layer  $r_o = r_{\text{top}}$  (radial distance of the LEO satellite). Then the electron density values at all latitudes ( $\varphi_o = -90, \dots, 270$ ) inside the top layer are determined by means of the observed TEC values  $T(r_{\text{top}}, \varphi_o, \delta_o)$ . Averaging of the calculated electron density values yields a complete row  $n_e(r_{\text{top}}, \varphi_o)$ , and Eq. (4) can be solved for the ionospheric layer below the top layer. This procedure is repeated until the base of the ionosphere at  $h = 60$  km is reached, so that a full slice of electron density has been computed from the TEC observations, with consideration of horizontal ionospheric gradients inside each layer. In practice we noted that high frequency oscillations of the electron density values (probably due to numerical errors) will increase from layer to layer. These oscillations are easily removed by smoothing each new calculated row of electron density with a sliding window average of  $10^\circ$  in latitude and 6 km in height before calculation of the next row.

The disadvantage of the 2-D recovery method is certainly a high error propagation during the recovery process of the  $n_e$ -field. Thus the TEC values should have small errors and should correspond to the same ionospheric state. Such problems also occur in case of radio tomography or data assimilation, and require improved data selection, preparation, error handling, and algorithms. Longitudinal variations of the ionosphere have been neglected in the present study. This might be justified for the ionosphere around noon and midnight.

### 3. Feasibility of 3-D Recovery of the Global Ionospheric Electron Density Distribution

The 2-D recovery method of the previous section can be easily extended to a 3-D recovery method, if a huge amount of GPS occultation data collected by a multi-satellite mission is available. The launch of the six satellite COSMIC mission in 2005 and numerous other radio occultation missions will lead to a high density of occultation events in space and time. One satellite may collect around 700 ionospheric occultations per day (Hajj *et al.*, 2000). Assuming 10 satellites this yields 7000 events per day. For derivation of an ionospheric climatology, data of two months, 60 days can be put together (e.g., derivation of the average diurnal variation of the global ionosphere in June/July). If the 3-D movie of the diurnal variation of the ionosphere is obtained by means of a 2-h sliding window in time, then we have  $(7000/12) \cdot 60$  or 35000 occultation events for each time step. At  $h = 400$  km the occultation density will be  $35000/(4\pi(6370 + 400)^2 \text{ km}^2)$  or  $6.1 \cdot 10^{-5}$  events/ $\text{km}^2$ . For each surface element of  $600 \text{ km} \times 600 \text{ km}$  (corresponding to  $5^\circ \times 5^\circ$ ) we will have in average around 22 events, corresponding to 22 TEC values  $T_k(r, \varphi_o, \vartheta_o, \delta_k)$ ,  $k = 1, 2, 3, \dots, 22$ .  $\varphi_o$  and  $\vartheta_o$  denote the latitude and longitude position of the surface element, and  $\delta_k$  are the viewing angles of the 22 occultation rays. This means 22 occultation rays are moving with their tangent point through the surface element. Almost the same is true for the surface elements beyond and below of 400 km height. Using a recursive formula such as Eq. (4) but with consideration of longitude as well, the electron density of the surface element can be determined 22 times, and the average will be taken. Our estimation shows that a 3-D recovery of the ionospheric climatology is feasible when 10 satellites with GPS

occultation receivers are in low Earth orbit.

An alternative 3-D tomographic solution of the whole equation matrix of all occultation rays possibly requires more computing efforts than our simple 3-D recovery method. Assuming a height step of 20 km the tomographic matrix of the example would require  $35000 \cdot (700 - 100)/20$  ( $>10^6$ ) equation lines for the ionosphere from 100 to 700 km. In so far our suggested 2-D and 3-D recovery method might be more feasible for a systematic extraction of the relevant information from a huge data set of ionospheric occultations. The advantage of a tomographic matrix solution is of course that this method can be applied to slanted rays and occultation rays. For occultation data alone a tomographic matrix solution is possibly not necessary.

#### 4. Abel Inversion

Contrary to the 2-D recovery method, the Abel inversion does not require a full slice of TEC values and has no error propagation along the latitudes. The Abel inversion is applied to each single TEC profile without consideration of horizontal gradients inside the layers. Equation (2) is simplified by

$$T(r_o) = 2 \int_{r_o}^{r_{\text{top}}} \frac{r n_e(r)}{\sqrt{r^2 - r_o^2}} dr. \quad (6)$$

The Abel transformation of this equation will give the electron density profile (Schreiner *et al.*, 1999; Tsai *et al.*, 2001; Hajj *et al.*, 2000)

$$n_e(r) = -\frac{1}{\pi} \int_r^{r_{\text{top}}} \frac{1}{\sqrt{r_o^2 - r^2}} \frac{dT(r_o)}{dr_o} dr_o. \quad (7)$$

Compared to Eq. (4) the number of numerical operations is quite similar for computation of a full slice of the ionosphere by Abel inversion. A retrieval error can occur if the electron density inside a layer changes with latitude or longitude which is illustrated in Fig. 1. In this figure the electron density value determined by ray A is used for analysis of ray B and C, though a different value would be required. However in case of a linear electron density gradient such as that of layer 2, the Abel inversion will retrieve the correct value at the tangent point, since the overestimation of electron density in the ray path segment on the left-hand-side (10 instead of 6) is canceled by the underestimation in the ray path segment on the right-hand-side (10 instead of 14). Retrieval errors occur for sharp maxima or minima of the latitudinal electron density distribution. In the following section the retrieval errors are visualized by retrieval of a meridional electron density slice from TEC data calculated for occultation ray paths through the IRI ionosphere.

#### 5. Retrieval Simulation Test with IRI-2001

The International Reference Ionosphere has been developed for more than 30 years and achieved a quite realistic description of the highly variable ionosphere for all conditions (Bilitza, 2001). Using IRI-2001 a meridional slice of electron density is computed for northern summer solstice 23 June 1995, 0:00 UT, geographic longitudes  $0^\circ$  (Greenwich, midnight) and  $180^\circ$  (noon) with  $1^\circ$ -spacing of electron density profiles. Then Eq. (2) is applied to transform the

$n_e(r_o, \varphi_o)$ -slice into the corresponding TEC slice  $T(r_o, \varphi_o)$ , so that all horizontal and vertical variations of the ionosphere along the ray paths are considered. The viewing angle  $\delta$  has been selected as zero that means the GPS rays are parallel to the meridian plane.

This is the starting point for application of both retrieval methods which are described in Sections 2 and 4. Figure 2(a) depicts the true IRI-2001 field of electron density which has to be reconstructed by the Abel inversion and the 2-D recovery method from the corresponding IRI-2001 TEC field. It is obvious that the IRI-2001 field contains many detailed structures, sometimes just  $10^\circ$  in latitude like over the south pole ( $-90^\circ$  or  $270^\circ$ ) or north pole ( $90^\circ$ ). The noon side ( $90$  to  $270^\circ$ ) is characterized by a strong enhancement of electron density near to the equator at  $180^\circ$ . The midnight side ( $-90$  to  $90^\circ$ ) shows an upward lifted F-layer and some wave structures. Because of northern summer the electron density of the northern hemisphere ( $0$ – $180^\circ$ ) is increased.

The reconstructed electron density field of the 2-D recovery method is shown in Fig. 2(b). The result is excellent for all heights beyond 200 km. Deviation from the true IRI-2001 field is less a few percent. All structures are recognized, in particular the sharp maxima over the poles and over the midnight equator ( $0^\circ$ ). Below 200 km height, we note some retrieval errors. These errors are due to the decreasing electron density below the F-layer. Small errors of retrieved electron density around the  $F_2$ -layer peak will significantly disturb the solutions at lower heights. A calibration of the retrieved electron density at the bottom of the ionosphere ( $n_e = 0$  at  $h = 60$  km) allows studies on the E region and might be considerable for improvement of the 2-D recovery method at heights below 200 km (e.g., Vorob'ev *et al.*, 1999; Hocke and Igarashi, 2002).

The result of the Abel inversion is depicted in Fig. 2(c). For illustration the path of one GPS ray through the ionosphere is shown by a white line. The GPS signal travels over a distance of  $40^\circ$  in latitude through the ionosphere at heights below 700 km. The ray path corresponds to a straight line in a cartesian coordinate system. On the first view, we can see that the Abel inversion smoothed out several small structures over the poles and the midnight equator. In addition the retrieval result of the equator anomaly at noon is not so good as for the 2-D recovery method. However the main characteristics of the IRI-2001 ionosphere are also recognized by the Abel inversion, and we can state that the Abel inversion makes a good job in spite of the non-spherical IRI-2001 ionosphere. The simulation represents the worst case for Abel inversion of occultation data of the noon and midnight ionosphere, since all ray paths are along the meridian plane where the horizontal (latitudinal) electron density variations are maximal.

#### 6. Results from GPS/MET and Comparison with IRI-2001

##### 6.1 Noon and midnight

In this section GPS/MET radio occultation data from the time interval June 19 to July 10, 1995 are analyzed. Geomagnetic activity was low to moderate during this time ( $K_p \sim 2$ – $3$ ). During this time the GPS signal encryption 'anti-spoofing' has been turned off, so that the GPS/MET

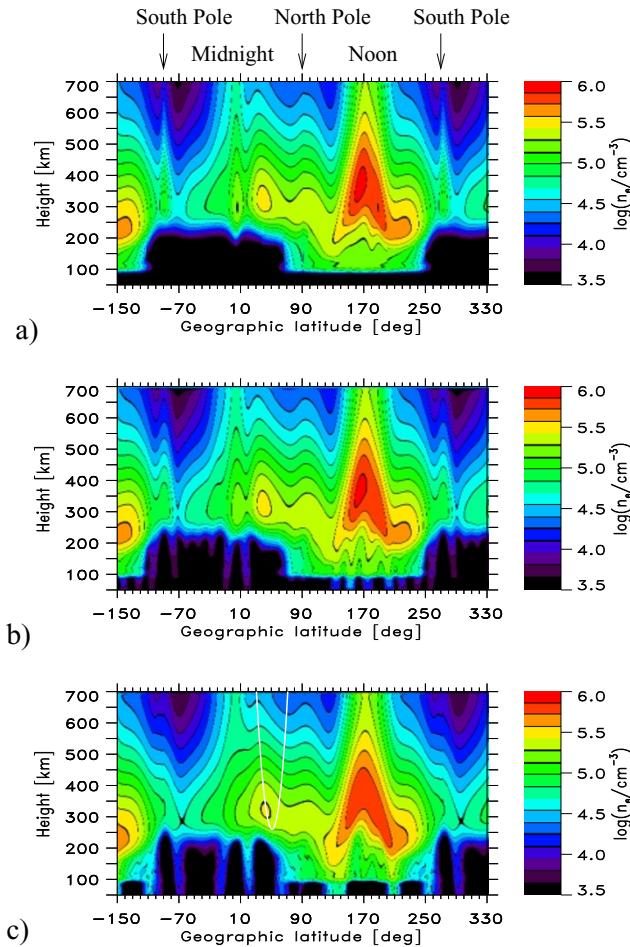


Fig. 2. Reconstruction test of a meridional electron density field from TEC data. a) True IRI-2001  $n_e$  field along the Greenwich meridian ( $0^\circ$  and  $180^\circ$  longitude) at midnight and noon at northern summer solstice 23 June 1995 (near to solar minimum), b) Retrieval result of the 2-D recovery method considering horizontal gradients, c) Retrieval result of the Abel inversion (with spherical symmetry assumption). The white line indicates a GPS-LEO ray path through the ionosphere.

measurements have a reduced phase path noise. In total 3495 occultations have been recorded in the F region. The sampling frequency of the phase path data is 0.1 Hz corresponding to a height resolution of around 20 km. By means of Eq. (1) TEC is derived from the phase path difference of the L1 and L2 signals. For each occultation the TEC values are represented as function of tangent point yielding a height profile of TEC.

The electron density profiles are recovered by the Abel inversion (Eq. (7)). The whole retrieval procedure has been performed by Dr. W. S. Schreiner from University Corporation for Atmospheric Research (UCAR). For calculation of a meridional slice the electron density profiles of the local times 10:00–14:00 LT and 22:00–2:00 LT are picked out and arranged as function of geomagnetic latitude. Then the profiles are averaged by a sliding window of  $15^\circ$  in latitude. Please note that these operations are necessary because of the lack of a sufficient amount of occultation data. Future satellite missions such as COSMIC (constellation of 6 micro-satellites) will provide a much better data base than the proof-of-concept mission GPS/MET. The average field

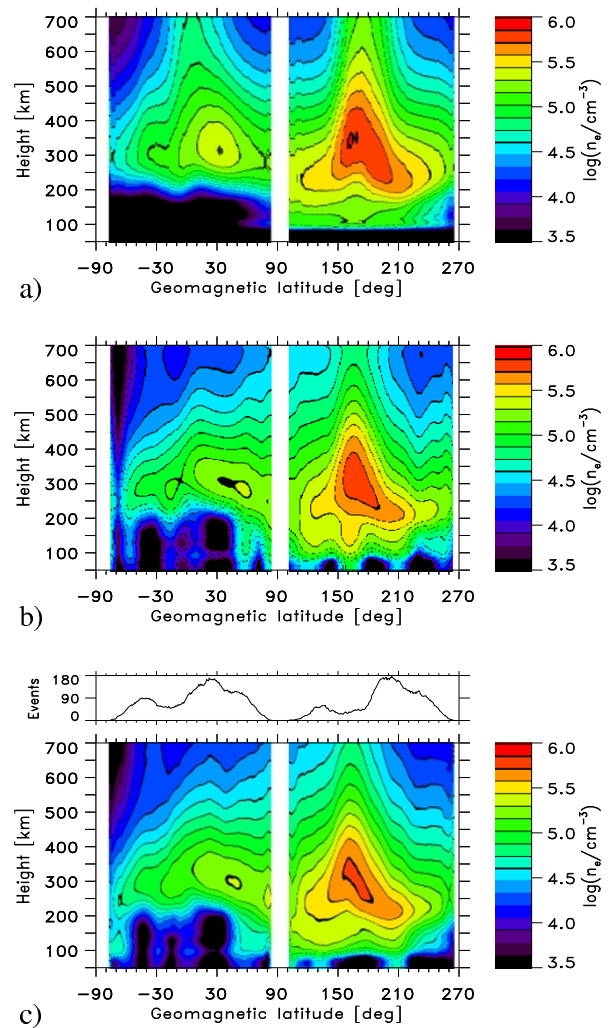


Fig. 3. Average meridional distribution of electron density as observed by GPS/MET radio occultation in June/July 1995 around noon (10:00–14:00 LT) and midnight (22:00–2:00 LT). a) IRI-2001 electron density field (electron density profiles have been calculated by IRI-2001 for the same places and times as given by the GPS/MET occultation events). b) Result of the 2-D recovery method. c) Result of the Abel inversion of electron density from TEC data of GPS/MET. Number of available occultation events per a latitude window of  $15^\circ$  are shown at the top.

of electron density is depicted in Fig. 3(c) for the Abel inversion. Figure 3(a) shows the corresponding IRI-2001 field where we averaged in the same manner IRI-2001 profiles calculated exactly at the same geographic places and times as given by the selected GPS/MET profiles used for Fig. 3(c).

The corresponding result of the 2-D recovery method are depicted in Fig. 3(b). The calculations have been performed by using Eqs. (3), (4), and (5). The inclination of Microlab-1's orbit is about  $70^\circ$ . The GPS antenna of Microlab-1 recorded occultations in anti-velocity direction of the spacecraft, so that we approximated the viewing angle  $\delta$  as  $20^\circ$ . The data gaps in the TEC field at the north and south pole have been filled by interpolation. These data gaps are a consequence of Microlab-1's orbit inclination of  $70^\circ$ , because the occultation places are less than around  $10^\circ$  away from the orbit. In case of the new radio occultation mission CHAMP the density of occultation events in the polar regions is excellent, since the orbit inclination of the CHAMP satellite has

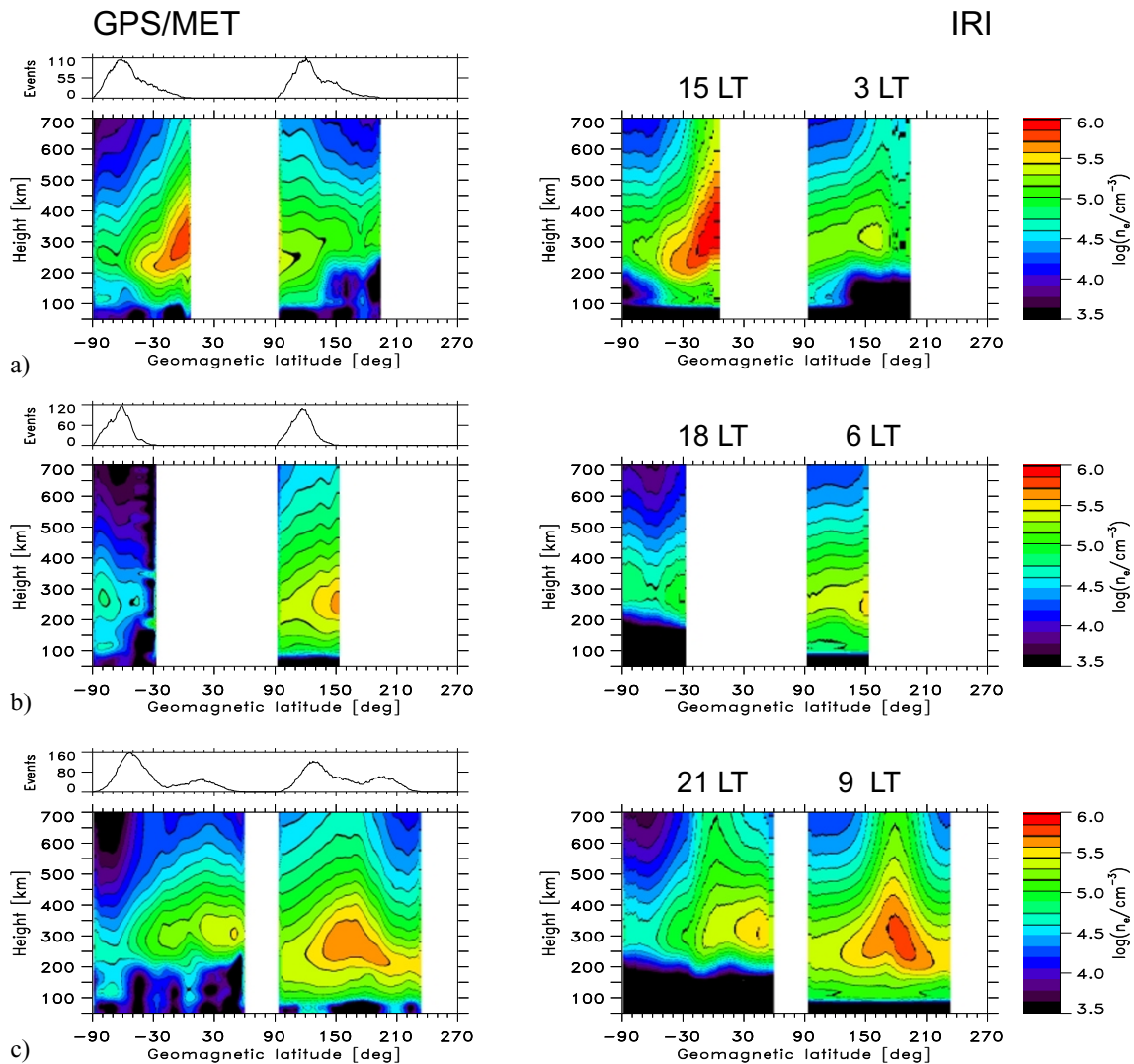


Fig. 4. Average meridional distributions of electron density for various local times in June/July 1995 (derived by Abel inversion). The northern summer hemisphere is always from 0 to 180° geomagnetic latitude. The IRI-2001 slices on the right-hand-side are calculated for the same times and places as the GPS/MET observations on the left-hand-side. The numbers of available occultation events (within a window of 15°) are shown in the upper panels of the viewgraphs on the left-hand-side, while the corresponding local times (3-h time window) are indicated on the right-hand-side.

been selected as 87.3°.

Comparing the result of the 2-D recovery method with the Abel inversion, it seems that its resolution is better at midnight. On the other hand, it seems that the 2-D recovery method generates higher errors than the Abel inversion in the  $F_1$  region at noon. We guess that the GPS/MET data set of June/July 1995 is not so appropriate for application of the 2-D recovery method. As mentioned before, this method has a higher sensitivity to errors than the robust Abel inversion. The errors could be due to data gaps at the poles and to the scatter of the occultation events over all longitudes and over 2–3 weeks. We already suppressed the scatter effect of the retrieved electron density values by removal of the lower and upper quartiles before calculation of the average electron density in the grid cells. Contrary to near-real-time tomography and data assimilation into space weather models, the checking of the observational data is easier for our statistical analysis, since the average electron density value and the standard deviation are defined for each grid cell. The different dependence of electron density on geographic and

geomagnetic coordinates may introduce further slight errors of the retrieved meridional slice. Details of the influences of various error sources and ambiguities on the 2-D recovery have to be addressed in a follow-on-study (e.g., impact of longitudinal variation of the ionosphere, small-scale structures, variability of solar radiation flux, and geomagnetic activity). A separate retrieval of electron density distributions for high and low geomagnetic activity might be more accurate and allows advanced comparisons to IRI.

Both recovery methods yield similar electron density values in the F region and topside ionosphere. The nighttime topside ionosphere observed by GPS/MET (Figs. 3(b), (c)) significantly deviates from IRI-2001 (Fig. 3(a)) which predicts an electron density maximum in the topside ionosphere at the geomagnetic equator (0°).

## 6.2 Other local times

The meridional coverage of available GPS/MET occultation events for June 19 to July 10, 1995 is best for the noon and midnight sectors, since the sun was within Microlab-1's orbit plane during this time interval. The precession of the

orbit plane relative to the sun is  $3.3^\circ/\text{day}$ , so that a time interval of around 55 days is required for a full coverage of all local times by GPS/MET (Schreiner *et al.*, 1998). Such a long time interval is not available for GPS anti-spoofing off observations during the GPS/MET mission. Consequently the derived meridional slices of other local times than noon and midnight have relative large data gaps. Because of these data gaps we can only use the Abel inversion. In spite of these limitations, the fragments of the meridional distributions of electron density at other local times are quite interesting since satellite-based ionosondes only provide the electron density distribution beyond the F layer maximum (Nava *et al.*, 2001). In addition to the meridional slice from noon to midnight (12 LT to 0 LT, Fig. 3), we select three other meridian planes rotated in steps of 3 LT or  $45^\circ$  longitude: a) from afternoon to after midnight (15 LT to 3 LT), b) from dusk to dawn (18 LT to 6 LT), and c) from after sunset to after sunrise (21 LT to 9 LT). The data window length is always 3 hours in time, and the electron density profiles have been averaged by a sliding window of  $15^\circ$  in latitude. The results are depicted for GPS/MET on the left-hand-side of Figs. 4(a), (b), (c) while the corresponding IRI-2001 slices are on the right-hand-side (obtained for IRI electron density profiles at the same places and times as the GPS/MET observations). The northern summer F region is shown at latitudes from  $0$  to  $180^\circ$ , while the southern winter F region is from  $-90$  to  $0^\circ$  or  $180$  to  $270^\circ$ .

Because of possible retrieval errors and data gaps our discussion is confined to the main characteristics. On the first view the GPS/MET and IRI results represent a similar diurnal variation of the ionosphere and a similar latitudinal dependence of electron density. As in Fig. 3, we note in Figs. 4(c), (a) a significant deviation of the nighttime equatorial topside ionosphere between the GPS/MET observations and IRI-2001. In Fig. 4(c) GPS/MET shows slight enhancements of electron density at 21 LT,  $30^\circ\text{N}$  and  $30^\circ\text{S}$  while IRI-2001 predicts a single and stronger enhancement in the F region beyond the geomagnetic equator (21 LT,  $0^\circ$ ,  $h = 400\text{--}700$  km). Since the Abel inversion is accurate for retrieval of electron density beyond the F layer maximum, we interpret this result as a significant departure between IRI and GPS/MET, observed for the nighttime topside ionosphere at low latitudes and near to solar minimum. In the same Fig. 4(c), a connection between the equatorial E region and F region is indicated by a thin vertical, green line. Though it is known that there are strong vertical plasma drifts in the equatorial ionosphere after sunset (cf. Kelley, 1989), we tend to interpret this feature as retrieval error of the Abel inversion due to the even structure formed by two electron density maxima at around  $h = 300$  km. As mentioned in Section 3 the Abel inversion fails for even (quadratic) variations of the ionosphere along the ray path. The two maxima are possibly due to electrodynamic lifting (prereversal enhancement) in the equatorial ionosphere after sunset.

The second significant departure from IRI-2001 occurs for the southern winter ionosphere at 18 and 21 LT (Figs. 4(b), (c)). The polar F-layer observed by GPS/MET is lower by about 50–100 km than the predicted IRI F-layer (at latitudes  $-60$  to  $-90^\circ$ ). Finally we like to draw the attention to the small ripples visible at 6 LT and 9 LT in the GPS/MET ob-

servations at heights 300 to 600 km (Figs. 4(b), (c)). This characteristic is even more obvious in the slices centered at 7 or 8 LT which are not shown here. These structures might be due to the disturbance of the thermosphere and ionosphere by the sudden sunrise at the dawn side (Galushko *et al.*, 1998; Somsikov and Ganguly, 1995). More occultation events measured around and after sunrise are required for an investigation of the spatial and temporal fluctuations at the solar terminator.

## 7. Summary and Outlook

A 2-D recovery method for retrieval of electron density from limb-sounding TEC data has been described. In case of an ideal simulation data set of IRI TEC data this method yields a superior horizontal resolution and accuracy compared to the Abel inversion. For the GPS/MET data set (June 19 to July 10, 1995) the advantages of this method are questionable, because of the high error propagation along the latitudes for a retrieval in presence of data gaps and TEC errors. TEC errors are possibly due to the scatter of the occultation events over 2–3 weeks and over all geomagnetic longitudes. These handicaps and retrieval errors generally exist for tomographic solutions and can be addressed by a better data preparation, error handling, and more observations. Checking of the data quality is easier for the 2-D recovery method than for near-real-time tomography. Mean value and standard deviation of the electron density values are defined at each grid cell for the 2-D recovery method. The data gaps in the polar regions disappear if the orbit inclination of the LEO satellite is sufficiently high (e.g.,  $87.3^\circ$  for CHAMP satellite). New occultation missions such as CHAMP, SAC-C, and COSMIC will generate continuous huge data sets for F region studies, and the 2-D recovery method can be extended to a 3-D recovery of the global ionosphere. A feasibility estimation shows that a 3-D recovery method is possibly appropriate for a systematic extraction of the relevant information from a huge amount of occultation rays and for determination of an ionospheric climatology without auxiliary data. On the other hand a conventional tomographic solution of the equation matrix of all occultation rays collected by a multi-satellite system within one or two months appears not feasible.

Comparison of meridional electron density slices observed by GPS/MET with those predicted by IRI-2001 gives a satisfactory agreement. Significant departures are detected for the nighttime topside ionosphere at low latitudes (around 21, 0, and 3 LT) and for the southern polar winter ionosphere (around 18–21 LT). These deviations are possibly due to a lack of traditional ionospheric observations at the geomagnetic equator and the southern polar region, and to the complexity of electrodynamic and magnetospheric processes in these regions. We conclude that the comparison between GPS/MET and IRI contributes to: 1) recognition of possible retrieval errors of the radio occultation method, 2) confirmation of results from IRI climatology and occultation observations, and 3) new aspects on the diurnal variation of the ionosphere on global scale. The potential of the 2-D recovery method is the improvement of the spatial resolution. In case of an appropriate radio occultation data set, the 2-D recovery method may resolve persistent small-scale structures

such as the ionospheric trough.

**Acknowledgments.** We are grateful to Dr. W. S. Schreiner (UCAR) who provided netCDF data files of the GPS/MET electron density profiles (retrieved by Abel inversion). We thank Dr. C. Rocken (UCAR) and the GPS/MET team for the GPS/MET experiment and discussions. The Telecommunications Advancement Organization (TAO) of Japan provided a research fellowship.

## References

- Bilitza, D., International Reference Ionosphere 2000, *Radio Sci.*, **36**, 261–275, 2001.
- Dymond, K. F. and R. J. Thomas, A technique for using measured ionospheric density gradients and GPS occultations for inferring the nighttime ionospheric electron density, *Radio Sci.*, **36**, 1141–1148, 2001.
- Galushko, V. G., V. V. Paznukhov, Y. M. Yampolski, and J. C. Foster, Incoherent scatter observations of AGW/TID events generated by the moving solar terminator, *Ann. Geophys.*, **16**, 821–827, 1998.
- Hajj, G. A., L. C. Lee, X. Pi, L. J. Romans, W. S. Schreiner, P. R. Straus, and C. Wang, COSMIC GPS ionospheric sensing and space weather, *Terr. Atmos. Ocean. Sci.*, **11**, 235–272, 2000.
- Hernández-Pajares, M., J. M. Juan, J. Sanz, and J. G. Solé, Global observation of the ionospheric electronic response to solar events using ground and LEO GPS data, *J. Geophys. Res.*, **103**, 20789–20796, 1998.
- Hocke, K. and K. Igarashi, Structure of the Earth's lower ionosphere observed by GPS/MET radio occultation, *J. Geophys. Res.*, **107**, 10.1029/2001JA900158, 2002.
- Kaplan, E. D., *Understanding GPS: Principles and Applications*, Artech House, Norwood, MA, 1996.
- Kelley, M. C., *The Earth's Ionosphere*, Academic Press, San Diego, 1989.
- Lee, L.-C., C. Rocken, and E. R. Kursinski (Eds), *Applications of Constellation Observing System for Meteorology, Ionosphere and Climate*, Springer-Verlag, Hong Kong, 384 pp., 2001.
- Leitinger, R., H.-P. Ladreiter, and G. Kirchengast, Ionosphere tomography with data from satellite reception of GNSS signals and ground reception of Navy Nav Satellite System signals, *Radio Sci.*, **32**, 1657–1669, 1997.
- Melbourne, W. G., E. S. Davis, C. B. Duncan, G. A. Hajj, K. R. Hardy, E. R. Kursinski, T. K. Meehan, and L. E. Young, The application of spaceborne GPS to atmospheric limb sounding and global change monitoring, *JPL Publication*, **94–18**, Jet Propulsion Laboratory, Pasadena, California, 1994.
- Mortensen, M. D., R. P. Linfield, and E. R. Kursinski, Vertical resolution approaching 100m for GPS occultations of the Earth's atmosphere, *Radio Sci.*, **34**, 1475–1484, 1999.
- Nava, B., S. M. Radicella, S. Pulinets, and V. Depuev, Modelling the bottom and topside electron density and TEC with profile data from topside ionograms, *Adv. Space Res.*, **27**(1), 31–34, 2001.
- Rius, A., G. Ruffini, and A. Romeo, Analysis of ionospheric electron-density distribution from GPS/MET occultations, *IEEE Trans. on Geoscience and Remote Sensing*, **36**(2), 383–394, 1998.
- Rocken, C., R. Anthes, M. Exner, D. Hunt, S. Sokolovskiy, R. Ware, M. Gorbunov, W. Schreiner, D. Feng, B. Herman, Y.-H. Kuo, and X. Zou, Analysis and validation of GPS/MET data in the neutral atmosphere, *J. Geophys. Res.*, **102**, 29849–28966, 1997.
- Schreiner, W. S., D. C. Hunt, C. Rocken, and S. V. Sokolovskiy, Precise GPS data processing for the GPS/MET radio occultation mission at UCAR, *Proc. of the Institute of Navigation - Navigation 2000*, 103–112, Alexandria, Va., 1998.
- Schreiner, W. S., S. V. Sokolovskiy, C. Rocken, and D. C. Hunt, Analysis and validation of GPS/MET radio occultation data in the ionosphere, *Radio Sci.*, **34**, 949–966, 1999.
- Somsikov, V. M. and B. Ganguly, On the mechanism of formation of atmospheric inhomogeneities in the solar terminator region, *J. Atmos. Terr. Phys.*, **57**, 75–83, 1995.
- Steiner, A., *High resolution sounding of key climate variables using the radio occultation technique*, Wiss. Bericht No. 3/1998, Inst. f. Meteorologie und Geophysik, University Graz, Austria, pp. 84–85, 1998.
- Tsai, L.-C., W.-H. Tsai, W. S. Schreiner, F. T. Berkey, and J. Y. Liu, Comparisons of GPS/MET retrieved ionospheric electron density and ground based ionosonde data, *Earth Planets Space*, **53**, 193–205, 2001.
- Vorob'ev, V. V., A. S. Gurvich, V. Kan, S. V. Sokolovskii, O. V. Fedorova, and A. V. Shmakov, Structure of the ionosphere based on radio occultation data from GPS 'Microlab-1' satellites: preliminary results, *Earth Obs. Rem. Sen.*, **15**, 609–622, 1999.
- Yakovlev, O. I., S. S. Matyugov, and I. A. Vilkov, Attenuation and scintillation of radio waves in the Earth's atmosphere from radio occultation experiments on satellite-to-satellite links, *Radio Sci.*, **30**, 591–602, 1995.

---

K. Hocke (e-mail: hocke@crl.go.jp) and K. Igarashi (e-mail: igarashi@crl.go.jp)